Cooperative Control of Unmanned Vehicles in a Time-Varying Flowfield

Cameron Peterson[*] and Derek A. Paley[†]

University of Maryland, College Park, MD, 20742, USA

Unmanned vehicles provide an effective approach for tracking, surveillance, and reconnaissance missions. Much work has been done to provide control algorithms to promote collaboration of UAVs and other autonomous vehicles. However, the majority of this work does not account for the adverse effects caused by flowfields. In this paper we present decentralized control algorithms designed to operate in a spatially or temporally varying flowfield. We use a Newtonian-particle model to represent each vehicle. Each particle travels at a constant speed and uses a steering control to compensate for the flow. We propose an algorithm that stabilizes a circular formation in a time-varying, spatially nonuniform flowfield. The center of the formation can be arbitrary or prescribed. In the case of a time-varying and spatially uniform flowfield, we propose an algorithm to stabilize a circular formation in which the temporal spacing between particles is regulated. The theoretical results are supported by numerical simulations that illustrate a circular formation tracking a maneuvering target as it turns or accelerates.

Nomenclature

N	Number of particles
r_k	Position of particle k
$\dot{r}_k$	Inertial velocity of particle k
s_k	Inertial speed of particle k at time t
$f_k(t)$	Flow velocity at position r_k and time t
θ_k	Orientation of the velocity of particle k relative to the flow
γ_k	Orientation of the inertial velocity of particle k
ψ_k	Time-phase of particle k
T	Period of revolution around a circular orbit
c_k	Center of circle traversed by particle k
ω_0	Constant angular rate
P	$N \times N$ projector matrix
P_k	kth row of matrix P
K	Control gain
i	Imaginary unit

Subscript

j, k	Particle and phase indices, $1, \ldots, N$

I.   Introduction

Autonomous vehicles provide a cost-effective, robust approach to tracking, surveillance and reconnaissance in land, air and sea. A cooperating team of vehicles can maximize the amount of collected information

---

[*]Graduate student, Department of Aerospace Engineering; `cammykai@yahoo.com`. AIAA Student Member.

[†]Assistant Professor, Department of Aerospace Engineering; `dpaley@umd.edu`. AIAA Senior Member.

by providing persistent, coordinated coverage of continuous and/or discrete spatiotemporal process. Unmanned platforms are ideal for multi-agent coordinated control of missions that require continuous area coverage with consistent revisit rates. Many algorithms are capable of providing stable, decentralized control of multiple agents with specific mobility and communication constraints.[1–9]

One obstacle limiting the operational efficacy of existing algorithms is their performance in the presence of an external flowfield. For some platforms, the flow speed may represent a significant fraction of the vehicle's inertial velocity. In a target-tracking application, motion of the target induces a flowfield in a reference frame fixed to the target. Therefore, a change in relative distance between a target and UAV could result from the influence of an external flowfield or from target motion. Although the results of this research are broadly applicable, we highlight their application to target tracking.

Some existing algorithms support operation in weak flowfields that are less than 10% of the platform speed relative to the flow. However, moderate (between 10% and 99%) and strong (100% or greater) flowfields present a significant challenge. This paper builds upon previous work in which decentralized control algorithms are presented for spatially varying, time-invariant flowfields.[10, 11] We consider spatially uniform or nonuniform flowfields that can be time-invariant or time-varying. We assume each vehicle senses the local flowfield and moves at unit speed relative to the flow.

We utilize a Lyapunov-based approach to design decentralized algorithms that stabilize circular formations in a time-varying flowfield. Previous works have used similar control designs. For example, Frew et al.[5] uses Lyapunov generated guidance vector fields to create loiter circles, driving vehicles to a desired stand off radius. These results are enhanced by Summers et al. with adaptive estimates to allow vehicle cooperation with a constant, unknown flow field.[6] In Nelson et al.[12] vector fields, used in combination with a sliding mode control drive a single vehicle along complex paths approximated with straight line and circular orbit segments. A high-gain inner-loop control on the autopilot compensates for wind disturbances and experimental results show a UAV able to keep on course in winds reaching 50% of the aircraft's controllable speed.

In designing the decentralized algorithms we first provide a control law to stabilize a circular formation about an arbitrary point in a time-varying spatially nonuniform flowfield. Then we introduce a symmetry-breaking particle that allows the formation center to be specified. The latter algorithm enables the particles to track maneuvering targets. Lastly, we provide a time-splay control law that regulates the temporal spacing of the particles in a circular formation in a time-varying, spatially uniform flowfield induced in a reference frame fixed to a constant speed, turning target.

The paper proceeds as follows. Section II examines the Newtonian-particle model used to simulate the autonomous vehicles and incorporate external flowfields. Section III develops Lyapunov-based circular control algorithms for spatially and temporally variable flowfields. Section IV provides performance results for circular configurations in a variety of flowfields indicative of the behavior of a maneuvering target. Section V contains a summary of the results and highlights some ongoing work.

II.   Dynamic Model of Vehicles in a Flowfield

We model each unmanned vehicle as a planar, self-propelled particle moving at unit speed relative to a spatially and temporally variable flowfield.[11] Each particle is steered by a control force perpendicular to the velocity relative to the flow. We consider N particles, denoting the individual particle positions as r_k, where $k \in \{1, \ldots, N\}$. The inertial velocity of the kth particle is denoted by $\dot{r}_k$. The particles do not accelerate tangentially to their path and thus move with unit velocity $e^{i\theta_k}$ relative to the flowfield. The flowfield at r_k and time t is denoted by $f_k(t) = f(r_k, t)$. The equations of motion for particle k are[11]

$$
\begin{aligned}
\dot{r}_k &= e^{i\theta_k} + f_k(t) \\
\dot{\theta}_k &= u_k.
\end{aligned}
\tag{1}
$$

We let γ_k equal the orientation of the inertial velocity of the kth particle and $s_k(t) = s(t, r_k, \gamma_k)$ denote its magnitude. The particle model can be written[11]

$$
\begin{aligned}
\dot{r}_k &= s_k(t)e^{i\gamma_k} \\
\dot{\gamma}_k &= \nu_k,
\end{aligned}
\tag{2}
$$

where $s_k(t) = |e^{i\theta_k} + f_k(t)|$ and $\gamma_k = \arg(e^{i\theta_k} + f_k(t))$. Note, we require $|f_k(t)| < 1 \ \forall \ k, t$, which ensures

American Institute of Aeronautics and Astronautics
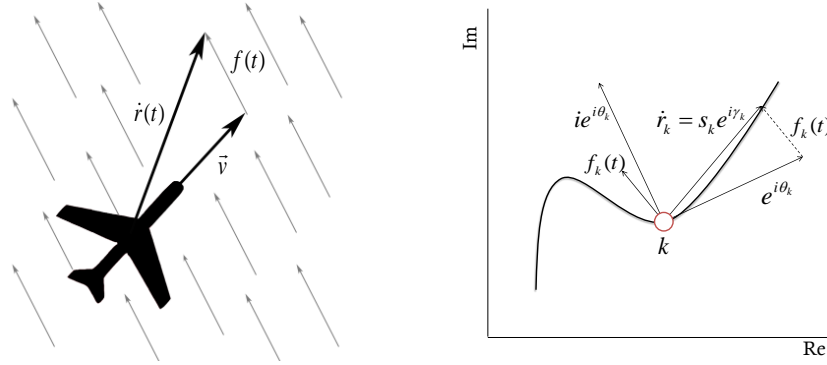
Figure 1. The inertial velocity of a particle is the sum of the flow velocity and the velocity of the particle relative to the flow.

$|s_k(t)| > 0$. From Figure 1 we see the following relationship[a] between θ_k and γ_k:

$$\sin \theta_k = s_k \sin \gamma_k - \langle f_k, i \rangle \tag{3}$$

$$\cos \theta_k = s_k \cos \gamma_k - \langle f_k, 1 \rangle, \tag{4}$$

which gives

$$\tan \gamma_k = \frac{\sin \theta_k + \langle f_k, i \rangle}{\cos \theta_k + \langle f_k, 1 \rangle}. \tag{5}$$

Differentiating (5) with respect to time and substituting in equations (3) and (4) yields

$$\dot{\gamma}_k = (\cos \theta_k \cos \gamma_k + \sin \theta_k \sin \gamma_k) s_k^{-1}(t) \dot{\theta}_k + \langle \dot{f}_k, i \rangle s_k^{-1}(t) \cos \gamma_k - \langle \dot{f}_k, 1 \rangle s_k^{-1}(t) \sin \gamma_k$$

$$= (1 - s_k^{-1}(t) \langle e^{i\gamma_k}, f_k \rangle) u_k + s_k^{-1}(t) \langle i e^{i\gamma_k}, \dot{f}_k \rangle \triangleq \nu_k, \tag{6}$$

where

$$\dot{f}_k = \frac{\partial f_k}{\partial r_k} \dot{r}_k + \frac{\partial f_k}{\partial t}. \tag{7}$$

Solving for u_k we obtain

$$u_k(t) = \frac{s_k(t) \nu_k - \langle i e^{i\gamma_k}, \dot{f}_k(t) \rangle}{s_k(t) - \langle e^{i\gamma_k}, f_k(t) \rangle}. \tag{8}$$

The resulting $u_k(t)$ is nonsingular since the denominator is never zero.[11] We calculate $s_k(t)$ and $u_k(t)$ in Example 1 for a time-varying, spatially uniform flowfield and, in Example 2, for a time-varying, spatially nonuniform flowfield.

Example 1. Time-varying, spatially uniform flowfield

Let a uniform flow be defined as $f(t) = \eta(t) e^{i\phi(t)}$, where $\eta(t)$ is the magnitude of the flow and $\phi(t)$ the direction. We drop the k subscript since a uniform flow at time t is identical for all particles. We constrain $|\eta(t)| < 1$, for all t, which ensure that $|s_k(t)| > 0$. We have

$$s_k(t) = \sqrt{\text{Re}\{(\eta(t) e^{i\phi(t)} + e^{i\theta_k})(\eta(t) e^{-i\phi(t)} + e^{-i\theta_k})\}}$$

$$= \sqrt{1 + (\eta(t))^2 + 2\eta(t)(\cos \theta_k \cos \phi(t) + \sin \theta_k \sin \phi(t))}. \tag{9}$$

We express $s_k(t)$ as a function of γ_k and $f(t)$ by substituting (3) and (4) into (9) and rearranging the result to obtain the quadratic equation

$$(s_k(t))^2 - 2\eta(t)(\cos \gamma_k \cos \phi(t) + \sin \gamma_t \sin \phi(t)) s_k(t) + (\eta(t))^2 - 1 = 0. \tag{10}$$

---

[a]We use the inner product $\langle x, y \rangle = \text{Re}\{\bar{x} y\}$, where $x, y \in \mathbb{C}$ and $\bar{x}$ is the complex conjugate of x.

Equation 10 has the solution (using the positive root since we require $s_k(t) > 0$),

$$s_k(t) = \eta(t)(\cos\gamma_k \cos\phi(t) + \sin\gamma_t \sin\phi(t)) + \sqrt{1 + (\eta(t))^2(\cos\gamma_k \cos\phi(t) + \sin\gamma_k \sin\phi(t) - 1)} \quad (11)$$
$$= \langle e^{i\gamma_k}, f(t)\rangle + \sqrt{1 - \langle ie^{i\gamma_k}, f(t)\rangle^2}. \quad (12)$$

We find $u_k(t)$ by substituting $f(t) = \eta(t)e^{i\phi(t)}$ and $\dot{f}(t) = \dot{\eta}(t)e^{i\phi(t)} + i\eta(t)\dot{\phi}(t)e^{i\phi(t)}$ into (8) to obtain

$$u_k(t) = \frac{\nu_k s_k(t) + \dot{\eta}(t)(\sin\gamma_k \cos\phi(t) - \cos\gamma_k \sin\phi(t)) + \eta(t)\dot{\phi}(t)(\sin\gamma_k \sin\phi(t) - \cos\gamma_k \cos\phi(t))}{s_k(t) - \eta(t)(\cos\gamma_k \cos\phi(t) - \sin\gamma_k \sin\phi(t))}. \quad (13)$$

Example 2. Time-varying, spatially nonuniform flowfield

For this example we let $f_k(t) = \beta_k(t) + i\alpha_k(t)$, where $\beta_k(t) = \beta(t, r_k)$ and $\alpha_k(t) = \alpha(t, r_k)$ are the real and imaginary components of the flowfield. Computing s_k yields

$$s_k(t) = \sqrt{\text{Re}\{(e^{i\theta_k} + \beta_k(t) + i\alpha_k(t))(e^{-i\theta_k} + \beta_k(t) - i\alpha_k(t))\}}$$
$$= \sqrt{1 - (\beta_k(t))^2 - (\alpha_k(t))^2 + 2s_k(t)(\alpha_k(t)\sin\gamma_k + \beta_k(t)\cos\gamma_k)}, \quad (14)$$

Next we express $s_k(t)$ as a function of γ_k and $f_k(t)$. Squaring both sides of (14) and solving the resulting quadratic equation (using the positive root since $s_k(t) > 0$) gives

$$s_k(t) = \alpha_k(t)\sin\gamma_k + \beta_k(t)\cos\gamma_k + \sqrt{1 - (\alpha_k(t)\cos\gamma_k - \beta_k(t)\sin\gamma_k)^2}$$
$$= \langle e^{i\gamma_k}, f_k(t)\rangle + \sqrt{1 - \langle ie^{i\gamma_k}, f_k(t)\rangle^2}. \quad (15)$$

To solve for $u_k(t)$ let the position of particle k be $r_k = x_k + iy_k$. The time-derivative of $f_k(t)$ is

$$\dot{f}_k(t) = \frac{\partial\beta_k}{\partial x_k}\dot{x}_k + \frac{\partial\beta_k}{\partial y_k}\dot{y}_k + \frac{\partial\beta_k}{\partial t} + i\left(\frac{\partial\alpha_k}{\partial x_k}\dot{x}_k + \frac{\partial\alpha_k}{\partial y_k}\dot{y}_k + \frac{\partial\alpha_k}{\partial t}\right).$$

Substituting $\dot{f}_k$ into (8) yields

$$u_k(t) = \frac{\nu_k s_k(t) - \sin\gamma_k\left(\frac{\partial\beta_k}{\partial x_k}\dot{x}_k + \frac{\partial\beta_k}{\partial y_k}\dot{y}_k + \frac{\partial\beta_k}{\partial t}\right) + \cos\gamma_k\left(\frac{\partial\alpha_k}{\partial x_k}\dot{x}_k + \frac{\partial\alpha_k}{\partial y_k}\dot{y}_k + \frac{\partial\alpha_k}{\partial t}\right)}{s_k(t) - \beta_k(t)\cos\gamma_k - \alpha_k(t)\sin\gamma_k}. \quad (16)$$

Thus, given γ_k, ν_k, $f_k(t)$, and $\dot{f}_k(t)$, one can always solve for $u_k(t)$, which is the control input to the original vehicle model (1).

III.   Stabilization of Circular Formations

In this section we provide decentralized control laws that stabilize a circular formation in a time-varying flowfield. We provide a control law to stabilize a circular formation about an arbitrary point in a spatially nonuniform flowfield. Then we introduce a symmetry-breaking particle that allows the formation center to be specified. The latter algorithm enables the particles to track maneuvering targets. We also provide a control law that regulates the spacing of the particles in a circular formation in a spatially uniform flowfield. In the next section, we illustrate these results in the context of tracking a maneuvering target.

III.A.   Circular Formation with an Arbitrary Center

We develop a control law that drives the particles into a circular formation about an arbitrary, fixed point. All of the particles in the circular formation travel in the same direction. In the case of a flow free environment, setting u_k equal to a constant ω_0 will drive the particles about a fixed center point with radius ω_0^{-1}. In the model (2), the center of a circular trajectory is[11]

$$c_k \triangleq r_k + \omega_0^{-1}i\frac{\dot{r}_k}{|\dot{r}_k|} = r_k + \omega_0^{-1}ie^{i\gamma_k}. \quad (17)$$

American Institute of Aeronautics and Astronautics

By differentiating (17) with respect to time we can derive a steering control ν_k that allows us to drive a single particle around a circle in a time-varying flow. We have

$$\dot{c}_k(t) = s_k(t)e^{i\gamma_k} - \omega_0^{-1}e^{i\gamma_k}\nu_k = (s_k(t) - \omega_0^{-1}\nu_k)e^{i\gamma_k}. \tag{18}$$

Equation (18) ensures $\dot{c}_k = 0$ when $\nu_k = \omega_0 s_k(t)$, which implies the center is fixed. Particle k will traverse a circle with radius given by $|\omega_0|^{-1} = |c_k(t) - r_k(0)|$.

Next we propose a steering control that drives all the particles to orbit the same center point in the same direction. Let $\mathbf{1} \triangleq (1,\ldots,1)^T \in \mathbb{R}^N$. In a circular formation, $c_k = c_j$ for all pairs j and k, which implies that a circular formation satisfies the condition $P\mathbf{c} = 0,^2$ where P is the $N \times N$ projection matrix given by

$$P = \text{diag}\{\mathbf{1}\} - \frac{1}{N}\mathbf{1}\mathbf{1}^T. \tag{19}$$

This matrix is equivalent to the Laplacian of an all-to-all communication topology. Since the intent of this paper is to focus on the time-varying aspect of the flow field we will assume only an all-to-all communication even though it may be possible to relax this constraint to a communication topology with limited connectivity.[3]

Consider the candidate Lyapunov function[2]

$$S(\boldsymbol{r},\boldsymbol{\gamma}) \triangleq \frac{1}{2}\langle \boldsymbol{c}, P\boldsymbol{c}\rangle. \tag{20}$$

We note that S is positive semi-definite. It is equal to zero only when $\boldsymbol{c} = c_0\mathbf{1}$, $c_0 \in \mathbb{C}$. The time derivative of S along solutions of (2) is

$$\dot{S} = \sum_{k=1}^{N}\langle \dot{c}_k, P_k\boldsymbol{c}\rangle = \sum_{k=1}^{N}\langle e^{i\gamma_k}, P_k\boldsymbol{c}\rangle(s_k(t) - \omega_0^{-1}\nu_k), \tag{21}$$

The following theorem extends [11, Theorem 3] to incorporate time-varying flow fields.

Theorem 1. Let $f_k(t) = f(r_k, t)$ satisfy $|f_k(t)| < 1$, $\forall\, k, t$. Choosing the control

$$\nu_k(t) = \omega_0(s_k(t) + K\langle P_k\boldsymbol{c}, e^{i\gamma_k}\rangle), \ K > 0, \omega_0 \neq 0 \tag{22}$$

forces uniform convergence of solutions of model (2) to the set of a circular formations with radius ω_0^{-1} and direction determined by the sign of ω_0.

Proof. The potential $S(\boldsymbol{r},\boldsymbol{\gamma})$ is radially unbounded and positive definite in the co-dimension one reduced space of relative centers. Under the control (22) the time derivative of S along solutions to (2) is

$$\dot{S} = -K\sum_{k=1}^{N}\langle P_k\boldsymbol{c}, e^{i\gamma_k}\rangle^2 \leq 0.$$

According to an invariance-like theorem for nonautonomous systems,[13] we see that the solutions of (2) with control (22) converge to the set $\{\dot{S} = 0\}$ in which

$$\langle P_k\boldsymbol{c}, e^{i\gamma_k}\rangle = 0, \ \forall\, k. \tag{23}$$

In this set, control (22) evaluates to $\nu_k(t) = \omega_0 s_k(t)$ and $\dot{c}_k = 0$, which implies each particle traverses a circle with a fixed center. Therefore, $P_k\boldsymbol{c}$ is constant and must be zero for (23) to hold. Since the null space of P is spanned by $\mathbf{1}$, then (23) is satisfield only when $P\boldsymbol{c} = 0$, which implies $c_k = c_j \ \forall\, k, j$. Since $\dot{S}$ is independent of time, the set of circular formations with radius ω_0^{-1} is uniformly asymptotically stable. $\qquad\square$

We illustrate the result in Figure 2 for a time-varying, spatially uniform flowfield and in Figure 3 for a time-varying, spatially nonuniform flowfield. Figure 2 illustrates a uniform flowfield directed along the real axis with sinusoidally varying magnitude $\eta(t) \leq 0.75$. The nonuniform flowfield depicted in Figure 3 is defined by the periodic function $f_k = a(t)(\sin(2\pi\omega x_k - \varphi_0) + i\cos(2\pi\omega y_k - \varphi_0))$, where $a(t) \leq 0.75$, $\omega = 1$, and $\varphi_0 = 10$.

American Institute of Aeronautics and Astronautics

(a) Uniform Flow, $t = 200$ s (b) Uniform Flow, $t = 400$ s (c) Uniform Flow, $t = 600$ s
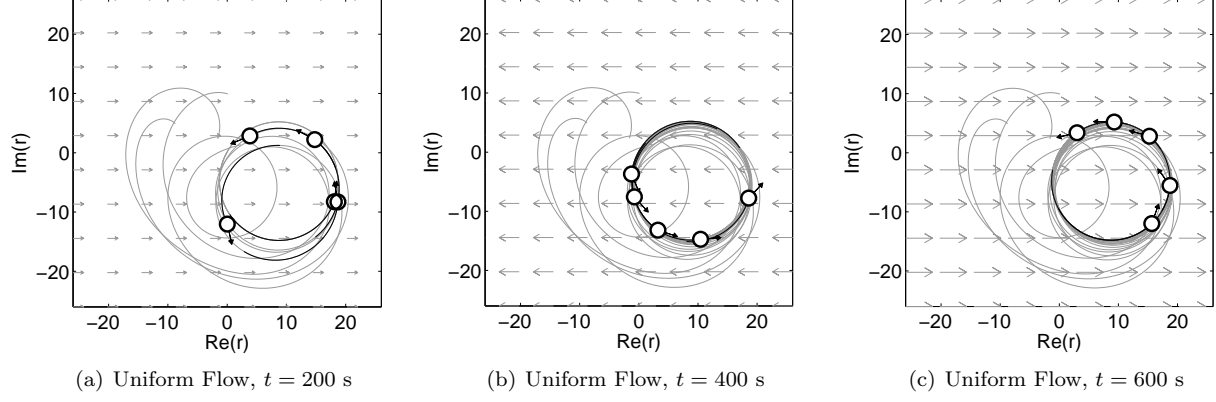
Figure 2. Stabilization of a circular formation with an arbitrary center in a time-varying, spatially uniform flowfield.

(a) Nonuniform Flow, $t = 200$ s (b) Nonuniform Flow, $t = 400$ s (c) Nonuniform Flow, $t = 600$ s
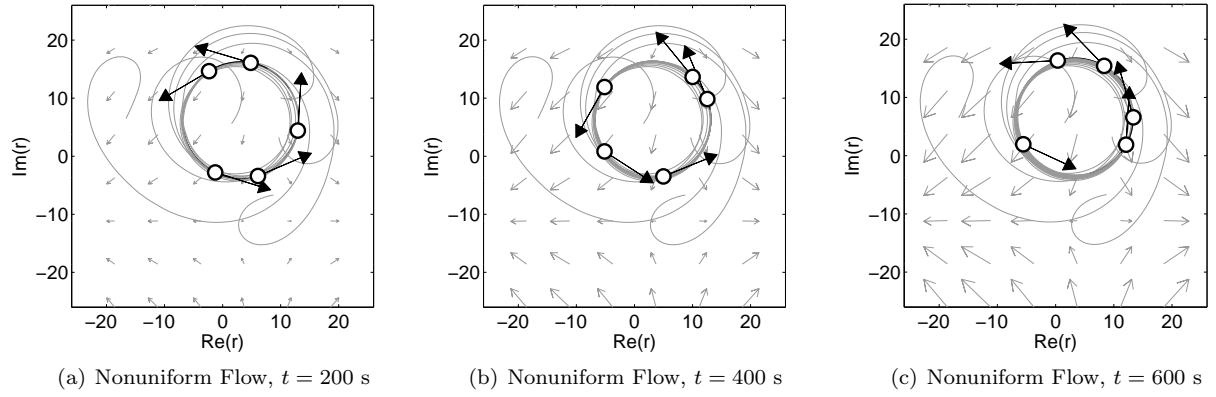
Figure 3. Stabilization of a circular formation with an arbitrary center in a time-varying, spatially nonuniform flowfield.

III.B. Circular Formation with a Prescribed Center

Under the control (22) the center of the circular formation depends only on the initial conditions of the particles. By introducing a virtual particle (indexed by $k = 0$) we can prescribe a center point for the formation, c_0, which is useful for applications including encirclement of a moving target.

Consider the augmented potential $\tilde{S}(\boldsymbol{r}, \boldsymbol{\gamma}) = S(\boldsymbol{r}, \boldsymbol{\gamma}) + S_0(\boldsymbol{r}, \boldsymbol{\gamma})$,[2] where

$$S_0(\boldsymbol{r}, \boldsymbol{\gamma}) = \frac{1}{2} \sum_{k=1}^{N} a_{j0} |c_k - c_0|^2, \tag{24}$$

Where $a_{k0} = 1$ if particle k is informed of the reference center, c_0, and $a_{k0} = 0$ otherwise. Taking the time-derivative of (24) gives

$$\dot{\tilde{S}} = \sum_{k=1}^{N} \left(\langle e^{i\gamma_k}, P_k \boldsymbol{c} \rangle + a_{k0} \langle e^{i\gamma_k}, c_k - c_0 \rangle \right) \left(s_k(t) - \omega_0^{-1} \nu_k \right) \tag{25}$$

The following theorem extends [11, Corollary 3] to incorporate time-varying flow fields.

Theorem 2. *Let* $f_k(t) = f(r_k, t)$ *satisfy* $|f_k(t)| < 1$, $\forall\, k, t$. *Choosing the control*

$$\nu_k(t) = \omega_0(s_k(t) + K(\langle e^{i\gamma_k}, P_k \boldsymbol{c} \rangle + a_{k0} \langle e^{i\gamma_k}, c_k - c_0 \rangle)), \ K > 0, \ \omega_0 \neq 0 \tag{26}$$

where $a_{k0} = 1$ *for at least one* $k \in 1, \dots, N$ *and zero otherwise, forces uniform convergence of all solutions of the model (2) to the set of circular formations centered on* c_0 *with radius* ω_0^{-1} *and direction determined by the sign of* ω_0.

American Institute of Aeronautics and Astronautics

Proof. The time-derivative of the augmented potential $\tilde{S}(\boldsymbol{r}, \boldsymbol{\gamma})$ satisfies

$$\dot{\tilde{S}} = -K \sum_{k=1}^{N} (\langle e^{i\gamma_k}, P_k \boldsymbol{c} \rangle + a_{k0} \langle e^{i\gamma_k}, c_k - c_0 \rangle)^2 \leq 0.$$

By an invariance-like principle for nonautonomous systems,[13] solutions of (2) converge to the set for which

$$\langle e^{i\gamma_k}, P_k \boldsymbol{c} \rangle + a_{k0} \langle e^{i\gamma_k}, c_k - c_0 \rangle = 0 \ \forall \ k. \tag{27}$$

If there exists a j such that, $a_{j0} = 0$, then (27) reduces to $\langle e^{i\gamma_j}, P_j \boldsymbol{c} \rangle$ and control (26) becomes $\nu_j(t) = \omega_0 s_j(t)$. The orientation of the inertial velocity, γ_j, is time-varying, therefore (27) holds for the uninformed particles only if $P_k \boldsymbol{c} = 0$, which implies that $\boldsymbol{c}$ is in the span of $\boldsymbol{1}$, i.e. $c_k = c_j$ for all pairs k and j. For the informed particles where $a_{k0} = 1$, (27) becomes

$$\langle e^{i\gamma_k}, c_k - c_0 \rangle = 0. \tag{28}$$

This is satisfied only if $c_k = c_0$ ensuring that all particles will converge to a circular formation around the prescribed center c_0.

If $a_{k0} = 1$, $\forall \ k$, then condition (27) reduces to

$$\langle e^{i\gamma_k}, \tilde{P}_k \tilde{\boldsymbol{c}} \rangle = 0, \ \forall \ k, \tag{29}$$

where $\tilde{P}$ is an $(N+1) \times (N+1)$ matrix as defined in (19) and $\tilde{\boldsymbol{c}} = [c_0, c_1, \ldots, c_N]^T$ is the vector of center positions augmented with the virtual particle's reference center, c_0. Condition (29) is satisfied only when $\tilde{\boldsymbol{c}}$ is in the span of $\tilde{\boldsymbol{1}}$, where $\boldsymbol{1} \triangleq (1, \ldots, 1)^T \in \mathbb{R}^{N+1}$ satisfying the circular formation condition and ensuring that $c_k = c_0 \ \forall \ k$. $\dot{\tilde{S}}$ is independent of time ensuring uniform asymptotic stability for all solutions to the model (2). $\qquad \square$

The examples given in Section IV illustrate the numerical results of this control.

III.C. Time-splay Circular Formation

In this section we derive a control algorithm that stabilizes a circular formation in which the temporal spacing between particles is regulated. We assume a spatially uniform flowfield of the form $f(t) = \eta_0 e^{i\Omega t}$, in which the magnitude $\eta(t) = \eta_0$ is constant and the direction $\phi(t) = \Omega t$ rotates at a constant rate Ω. Such a flowfield arises in a reference frame fixed to a constant-speed target that turns at a constant rate.

From (18) we know that $\nu_k = \omega_0 s_k$ drives particle k in a fixed circle of radius ω_0^{-1}. Consider the change of variables $\gamma_k' = \gamma_k - \Omega t$, which implies

$$\dot{\gamma}_k' = \dot{\gamma}_k - \Omega = \omega_0 s_k - \Omega. \tag{30}$$

Using (12), we obtain the following expression for s_k, which does not depend explicitly on time:

$$s_k = \eta_0 \cos \gamma_k' + \sqrt{(1 - \eta_0^2 \sin^2 \gamma_k')}. \tag{31}$$

For the ensuing calculations to be nonsingular, we require that (30) not have a fixed point. We ensure $\dot{\gamma}_k' > 0$ by requiring

$$\min_{\gamma'} s(\gamma') > \frac{\Omega}{\omega_0}. \tag{32}$$

The minimum of s_k in (31) is $s_k = 1 - \eta_0$ which occurs for $\gamma_k' = \pi$. Thus, the constraint (32) is equivalent to

$$\omega_0 > \frac{\Omega}{1 - \eta_0}. \tag{33}$$

Note (33) establishes a lower bound on the minimum formation radius of $|\omega_0|^{-1} = (1 - \eta_0)/\Omega$. Substituting (31) into (30) and integrating by separation of variables yields

$$t = \int_0^{\gamma_k'(t)} \frac{d\gamma'}{\omega_0 s(\gamma') - \Omega}. \tag{34}$$

We use a quantity called the *time-phase* to regulate the time separation of the N particles.[11] The time-phase for a time-varying, uniform flow $f(t) = \eta_0 e^{i\Omega t}$ is

$$\psi_k = \frac{2\pi}{T} \int_0^{\gamma_k'(t)} \frac{d\gamma'}{\omega_0 s(\gamma') - \Omega}, \tag{35}$$

where T, the period of a single revolution, is

$$T = \int_0^{2\pi} \frac{d\gamma'}{\omega_0 s(\gamma') - \Omega}. \tag{36}$$

The time-derivative of (35) is

$$\dot{\psi}_k = \frac{2\pi}{T} \frac{\nu_k - \Omega}{\omega_0 s_k - \Omega}. \tag{37}$$

Note (37) implies that the control $\nu_k = \omega_0 s_k$ yields $\dot{\psi}_k = 2\pi/T$, which is constant. To stabilize a circular formation in which the relative time-phases are regulated, we consider the composite potential[2]

$$V(\boldsymbol{r}, \boldsymbol{\gamma}) = S(\boldsymbol{r}, \boldsymbol{\gamma}) + \frac{T}{2\pi} U(\boldsymbol{\psi}). \tag{38}$$

The phase potential $U(\boldsymbol{\psi})$ is a smooth function satisfying the rotational symmetry property $U(\boldsymbol{\psi} + \psi_0 \mathbf{1}) = U(\boldsymbol{\psi})$, which implies[2]

$$\sum_{k=1}^N \frac{\partial U}{\partial \psi_k} = 0. \tag{39}$$

Using (39) and (37), we obtain the time-derivative of the potential (38),

$$
\begin{aligned}
\dot{V} &= \sum_{k=1}^N \langle e^{i\gamma_k}, P_k \boldsymbol{c} \rangle (s_k - \omega_0^{-1} \nu_k) + \frac{T}{2\pi} \frac{\partial U}{\partial \psi_k} \dot{\psi}_k \\
&= \sum_{k=1}^N \left(s_k \langle e^{i\gamma_k}, P_k \boldsymbol{c} \rangle - \frac{\partial U}{\partial \psi_k} \frac{\omega_0 s_k}{\omega_0 s_k - \Omega} \right) \left(\frac{\omega_0 s_k - \nu_k}{\omega_0 s_k} \right).
\end{aligned} \tag{40}
$$

The following theorem extends [11, Theorem 5] to incorporate time-varying flow fields.

Theorem 3. *Let $f(t) = \eta_0 e^{i\Omega t}$ be a spatially invariant flow field satisfying the condition $|\eta_0| < 1$, $\forall\, t$. Also, let $U(\psi)$ be a smooth, rotationally symetric phase potential. Choosing the control*

$$\nu_k = \omega_0 s_k \left(1 + K \left(s_k \langle e^{i\gamma_k}, P_k \boldsymbol{c} \rangle - \frac{\partial U}{\partial \psi_k} \frac{\omega_0 s_k}{\omega_0 s_k - \Omega} \right) \right), \quad K > 0, \omega_0 \neq 0 \tag{41}$$

stabilizes a circular formation with radius ω_0^{-1} and direction determinmed by the sign of ω_0 in which the time-phase arrangement is a critical point of $U(\boldsymbol{\psi})$.

Proof. Using control (41) with potential (40) yields

$$
\begin{aligned}
\dot{V} &= -K \sum_{k=1}^N \left(s_k^2 \langle e^{i\gamma_k}, P_k \boldsymbol{c} \rangle^2 - 2 \frac{\partial U}{\partial \psi_k} \frac{\omega_0 s_k}{\omega_0 s_k - \Omega} \langle e^{i\gamma_k}, P_k \boldsymbol{c} \rangle + \left(\frac{\partial U}{\partial \psi_k} \frac{\omega_0 s_k}{\omega_0 s_k - \Omega} \right)^2 \right) \\
&= -K \sum_{k=1}^N \left(s_k \langle e^{i\gamma_k}, P_k \boldsymbol{c} \rangle - \left(\frac{\partial U}{\partial \psi_k} \frac{\omega_0 s_k}{\omega_0 s_k - \Omega} \right) \right)^2 \leq 0
\end{aligned} \tag{42}
$$

By an invariance-like principle for non-autonomous systems,[13] solutions of (2) converge to the set $\{\dot{V} = 0\}$ for which

$$s_k \langle e^{i\gamma_k}, P_k \boldsymbol{c} \rangle - \frac{\partial U}{\partial \psi_k} \frac{\omega_0 s_k}{\omega_0 s_k - \Omega} = 0, \tag{43}$$

American Institute of Aeronautics and Astronautics

(a) Uniform Flow, $t = 500$ s   (b) Uniform Flow, $t = 1000$ s   (c) Uniform Flow, $t = 1500$ s
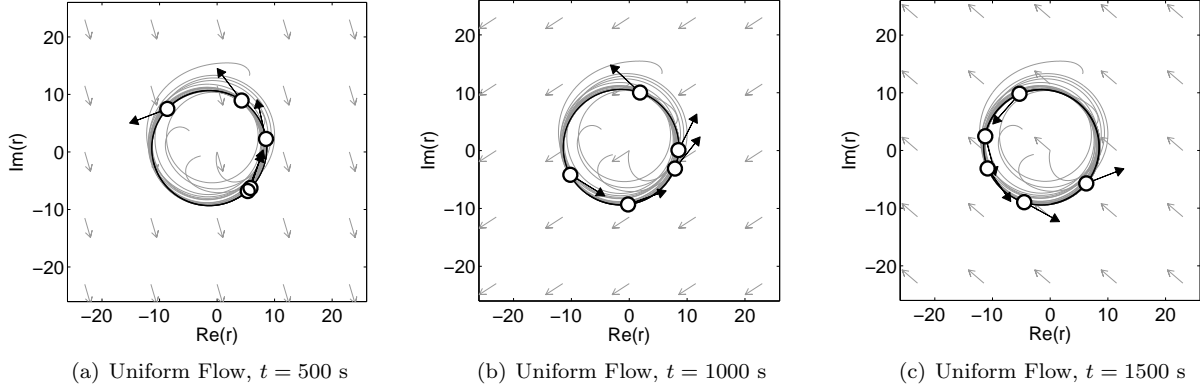
Figure 4. Stabilization of a time-splay formation with an arbitrary center in a time-varying, spatially uniform flowfield.

for $k = 1, ..., N$. By (41), we see that in this set, $\nu_k = \omega_0 s_k$. Thus each particle travels around a circle with a fixed center and radius $|\omega_0|^{-1}$. Also $\dot{\psi}_2 = 2\pi/T$, which implies that $U(\boldsymbol{\psi})$ is constant (by (39)) and $\frac{\partial U}{\partial \psi_k} = 0 \; \forall \; k$. Constraint (42) reduces to

$$\langle e^{i\gamma_k}, P_k \boldsymbol{c} \rangle = 0. \tag{44}$$

$P_k \boldsymbol{c}$ is constant and must be zero for (44) to hold. The null space of P is spanned by $\mathbf{1}$, therefore (44) is satisfied only when $P\boldsymbol{c} = 0$, which implies $c_k = c_j \; \forall \; k, j$. Since $\dot{V}$ is independent of time, the set of circular formations with radius ω_0^{-1} is uniformly asymptotically stable. $\qquad\square$

Theorem 3 establishes convergence to a critical point of a rotationally symmetric potential $U(\boldsymbol{\psi})$. Choosing the (M,N)-potential $U^{M,N}$ defined as[2]

$$U^{M,N}(\boldsymbol{\psi}) = \sum_{m=1}^{M} K_m U_m \tag{45}$$

where

$$U_m(\boldsymbol{\psi}) = \frac{N}{2}|p_{m\psi}|^2, \; p_{m\psi} \triangleq \frac{1}{mN}\sum_{k=1}^{N} e^{im\psi_k}.$$

renders the set of time-splay formations uniformly asymptotically stable, since they are the minimum of $U^{M,N}$. Note that $K_m > 0$ for $m = 1, \ldots, N-1$, and $K_N < 0$.

We illustrate Theorem 3 in Figure 4, showing $N = 5$ particles as they converge to a time-splay configuration for a time-varying, spatially uniform flow field of the form $f(t) = \eta_0 e^{i\Omega t}$. Setting parameters $\eta_0 = 0.5$ and $\Omega = 0.01$ and choosing $\omega_0 = 0.1$ ensures that the constraint (33) is satisfied.

Introducing a virtual particle as in the previous section enables the center of the time-splay formation to be prescribed.

Corollary 1. *Let $a_{k0} = 1$ if particle k is informed of the reference center, c_0, and $a_{k0} = 0$ otherwise. Let $f(t) = \eta_0 e^{i\Omega t}$ be a spatially invariant flow field satisfying the condition $|\eta_0| < 1$, $\forall \; t$. Also, let $U(\psi)$ be a smooth, rotationally symetric phase potential. Choosing the control*

$$\nu_k = \omega_0 s_k \left(1 + K \left(s_k \left(\langle e^{i\gamma_k}, P_k \boldsymbol{c} \rangle + a_{k0} \langle e^{i\gamma_k}, c_k - c_0 \rangle \right) - \frac{\partial U}{\partial \psi_k} \frac{\omega_0 s_k}{\omega_0 s_k - \Omega} \right) \right), \; K > 0, \omega_0 \neq 0 \tag{46}$$

where $a_{k0} = 1$ for at least one $k \in 1, \ldots, N$ and zero otherwise, stabilizes a circular formation centered on c_0 with radius ω_0^{-1} and direction determined by the sign of ω_0 in which the time-phase arrangement is a critical point of $U(\boldsymbol{\psi})$.

Corollary 1 is illustrated in Section IV with Figure 7.

American Institute of Aeronautics and Astronautics

(a) Target-Centered, $t = 400\ s$ (b) Target-Centered, $t = 600\ s$ (c) Inertial Frame
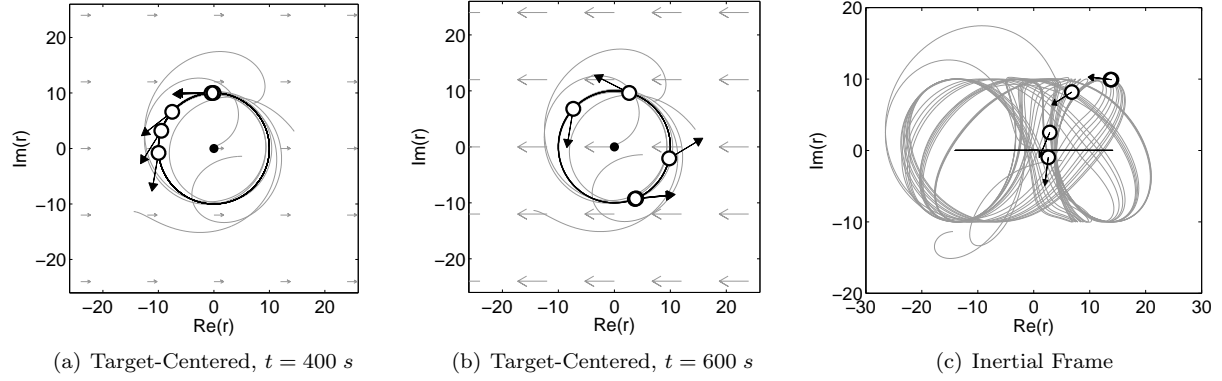
Figure 5. Encirclement of a maneuvering target that is accelerating without turning.

IV. Application Example: Encirclement of a Maneuvering Target

In this section we consider the scenario of multiple unmanned vehicles tracking a maneuvering target. We define a non-rotating reference frame $\mathcal{B}$ whose origin is fixed to the target. When the equations of motion (2) are expressed in frame $\mathcal{B}$, the motion of the target yields a spatially uniform flow $f(t) = \eta(t)e^{i\phi(t)}$. We utilize the control laws developed in III to assign the center point of the circular formation to the target.

We illustrate the target tracking scenario with three examples. First, we consider a target that is continuously accelerating and decelerating without turning. The magnitude of the velocity is always changing, but the direction is constant. The second example illustrates the coordinated encirclement of a target that is traversing a circle of fixed radius and thus constantly changing its velocity direction while maintaining a fixed magnitude. This example exemplifies a flowfield that rotates at a constant rate as prescribed in Section III.C. For this flowfield, we use the time-phase parameter to regulate the temporal spacing of the particles. All of the examples illustrate realistic maneuvers of a ground vehicle.

IV.A. Coordinated Encirclement of a Variable-Speed Target

This example replicates a target that is accelerating and decelerating along a single direction. Since the flowfield is uniform and only varies in magnitude, we can align $f(t) = \eta(t)e^{i\phi_0}$ with the positive real axis, without loss of generality. We illustrate this scenario with the following flowfield

$$\eta(t) = \begin{cases} \frac{4At}{T} - A, & t < \frac{T}{2} \\ \frac{-4A(t - \frac{T}{2})}{T} + A, & t \geq \frac{T}{2}, \end{cases} \tag{47}$$

where A and T characterize the target behavior by representing the maximum amplitude and the period respectively. The target velocity is strongest in the middle portion of the track and gradually slows down and reverses direction at the edges. This cycle is repeated for the desired time span of the simulation.

Figure 5 illustrates the tracking result of a target traversing with a maximum velocity of $A = 0.75$ and period $T = 150$. Figures 5(a) and 5(b) shows the UAVs in frame $\mathcal{B}$, which is centered on the target. This depicts the quick convergence of the targets to the circular formation. Figure 5(c) shows the simulation results in an inertial reference frame. The target is aligned with the real axis and travels left and right without turning.

IV.B. Coordinated Encirclement of a Turning Target

In this example, we study the behavior of the particles as they follow a target performing a continuous circular turn. In the target-fixed frame, $\mathcal{B}$, there is a time-varying, uniform flowfield $f(t) = \eta_0 e^{i\phi(t)}$, which has a fixed magnitude, η_0. The flow direction is $\phi(t) = (\eta_0/\rho)t$, where ρ is the radius of curvature of the target trajectory. Figure 6 illustrates the results of using control algorithm (26) with speed $\eta_0 = 0.8$ and radius of curvature $\rho = 63.66$. Figures 6(a) and 6(b) display the simulation results in a target-fixed frame. Figure 6(c) illustrates the results in an inertial frame that is not translating with the target.

American Institute of Aeronautics and Astronautics

(a) Target-Centered, $t = 400\ s$ (b) Target-Centered, $t = 800\ s$ (c) Inertial Frame
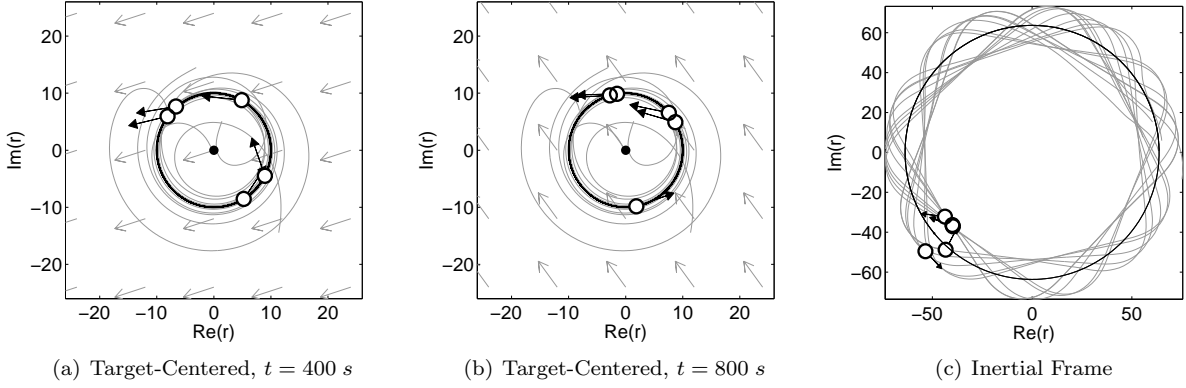
Figure 6. Encirclement of a maneuvering target that is turning at a constant rate.

(a) Target-Centered, $t = 800\ s$ (b) Target-Centered, $t = 1000\ s$ (c) Inertial Frame
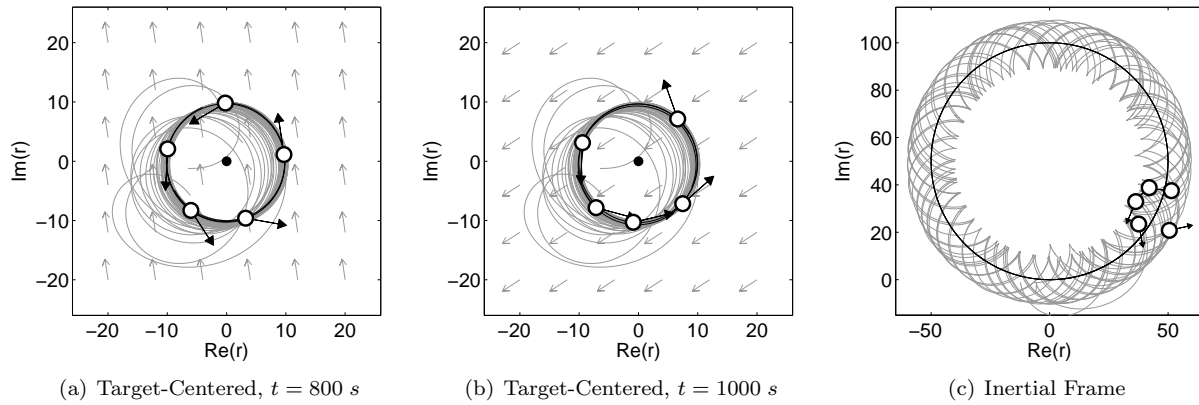
Figure 7. Coordinated encirclement of a maneuvering target that is turning at a constant rate.

We also use the turning target scenario to illustrate the control law (41), which drives the particles to a time-splay formation. Figure 7 illustrates this example with $N = 5$ particles centered on a target cycling at an angular rate of $\Omega = 0.01$. We set $\omega_0 = 0.1$ in order to satisfy requirement (33). This ensure that the turning radius of the target will be greater than the radius of the encircling air vehicles. The target speed is $\eta_0 = 0.5$. Figures 7(a) and 7(b) show the convergence to the time-splay configuration in the target-centered reference frame, $\mathcal{B}$. Figure 7(c) depicts the target and particles in an inertial frame.

V. Conclusions

Cooperative control improves the capability of autonomous vehicles to gather information, track targets and perform necessary mission objectives. In this paper, we present decentralized control algorithms that regulate the formation of autonomous vehicles while operating in a spatiotemporal flowfield. We represent the vehicle dynamics with a Newtonian-particle model in which each particle travels at unit speed. A steering control is applied perpendicular to the particle velocity relative to the flow. Decentralized control algorithms are proposed that stabilize circular formations in temporally and spatially varying flowfields. A solution that stabilizes a time-splay configuration for a specific set of time-varying flow fields is also proposed. Numerical results illustrate the capability to cooperatively encircle maneuvering targets that turn and accelerate. In ongoing work we seek to expand the class of flowfields in which the time-splay results apply. We will also investigate methods of coordinating multiple vehicles in an unknown flowfield.

American Institute of Aeronautics and Astronautics

References

[1]Justh, E. W. and Krishnaprasad, P. S., "Equilibria and Steering Laws for Planar Formations," *Systems and Control Letters*, Vol. 52, No. 1, 2004, pp. 25–38.

[2]Sepulchre, R., Paley, D. A., and Leonard, N. E., "Stabilization of planar collective motion: All-to-all communication," *IEEE Trans. Automatic Control*, Vol. 52, No. 5, 2007, pp. 811–824.

[3]Sepulchre, R., Paley, D. A., and Leonard, N. E., "Stabilization of planar collective motion with limited communication," *IEEE Trans. Automatic Control*, Vol. 53, No. 3, 2008, pp. 706–719.

[4]Elston, J. and Frew, E., "Unmanned Aircraft Guidance for Penetration of Pre-Tornadic Storms," *Proc. AIAA Guidance, Navigation and Control Conf. and Exhibit (electronic)*, No. AIAA-2008-6513, Honolulu, Hawaii, 2008, (16 pages).

[5]Frew, E. W., Lawrence, D. A., and Morris, S., "Coordinated Standoff Tracking of Moving Targets Using Lyapunov Guidance Vector Fields," *J. Guidance, Control, and Dynamics*, Vol. 31, No. 2, 2008, pp. 290–306.

[6]Summers, T. H., Akella, M. R., and Mears, M. J., "Coordinated Standoff Tracking of Moving Targets: Control Laws and Information Architectures," *J. Guidance, Control, and Dynamics*, Vol. 32, No. 1, 2009, pp. 56–69.

[7]Olfati-Saber, R. and Murray, R., "Graph Rigidity and Distributed Formation Stabilization of Multi-Vehicle Systems," *IEEE Conference on Decisions and Control*, 2002.

[8]Kingston, D. B., *Decentralized Control of Multiple UAVs for Perimeter and Target Surveillance*, Ph.D. thesis, Department of Electrical and Computer Engineering, Brigham Young University, Provo, Utah, December 2007.

[9]Fax, J. A. and Murray, R. M., "Information Flow and Cooperative Control of Vehicle Formations," *IEEE Trans. Automatic Control*, Vol. 49, No. 9, 2004, pp. 1465–1476.

[10]Paley, D. A., "Stabilization of Collective Motion in a Uniform and Constant Flow Field," *Proc. AIAA Guidance, Navigation and Control Conf. and Exhibit*, No. AIAA-2008-7173, Honolulu, Hawaii, August 2008, (8 pages).

[11]Paley, D. A. and Peterson, C., "Stabilization of Collective Motion in a Time-Invariant Flow Field," *J. Guidance, Control, and Dynamics*, Vol. 32, No. 3, 2009, pp. 771–779.

[12]Nelson, D. R., Barber, D. B., and Beard, R. W., "Vector Field Path Following for Miniature Air Vehicles," *IEEE Transactions on Robotics*, Vol. 23, June 2007, pp. 519–529.

[13]Khalil, H. K., *Nonlinear Systems*, Prentice Hall, 3rd ed., 2002.